

Modeling and Computation of Nanoparticles in Fluid Flow: Plasma Flow Synthesis

Pierre Proulx, ing. Ph.D., professor *
Department of chemical engineering, Universite de Sherbrooke

February 9, 2009

Contents

1	Plasma flow synthesis	3
1.1	Introduction	3
1.2	The Inductively Coupled Plasma (ICP)	5
1.3	ICP production of nanoparticles	6
1.4	Plasma properties	6
1.4.1	Thermodynamic properties	6
1.4.2	Transport properties	9
1.5	CFD equations specific to thermal plasmas	13
1.5.1	Thermal equilibrium	13
1.5.2	Thermal non-equilibrium	13
1.5.3	Auxiliary relations	16
1.5.4	Radiation	17
1.5.5	Vector potential equations	18
1.6	Application of the equilibrium model model	19
1.6.1	Computational domain and boundary conditions	19
1.6.2	Results	21
1.7	Conclusion	21

*The author wishes to acknowledge the contribution of his graduate students: B. M. Goortani, N.-Y. M. Gonzalez, S. Xue, D. Pelletier, M. Elmorsli, A. Bannari, R. Bannari, B. Selma and his colleagues F. Gitzhofer, J. Jurewicz and D. Gravelle and M. I. Boulos.



1 Thermal plasmas synthesis of nanoparticles

1.1 Introduction

Thermal plasmas are partially or strongly ionized gases, usually created by electric arcs at atmospheric pressure. In fact, thermal plasmas can be generated by many methods, such as direct electrical discharges at current intensities varying from a few amperes and up to hundreds of amperes, free burning arcs and transferred arcs, non-transferred plasma torches, either AC or transient arcs and lamps, circuit-breakers, pulsed arcs, RF and microwave discharges, as well as laser induced plasmas in expansion phase. In the following text, thermal plasmas will be essentially treated as very hot gases. They are often qualified as thermal if they are close to, or in LTE (Local Thermodynamic Equilibrium). This state of equilibrium is obtained when the pressure in the plasma is sufficient to ensure that the energy is equipartitioned between all molecular and atomic excited states, but not high enough to ensure that the plasma emits as a blackbody. It is generally accepted (or at least tolerated) to say that plasma torches operating close to atmospheric pressure are close to LTE except near the fringes of the plasma where the stronger gradients exist. As a consequence, in order to obtain a valid description of a DC or a transferred arc plasma torch, even with the LTE assumption one must take into account the non-LTE behavior of the plasma near the electrodes. The rf inductively coupled plasma (ICP) is somehow different, since it has no electrode directly in contact with the plasma.

In thermal plasmas, the electrons are mainly responsible for inelastic collisions, such as ionization, recombination, excitation, de-excitation, attachment, and detachment. Due to the high value of the electron density, the inelastic collision frequencies are high, and thus tend to establish a statistical equilibrium among all particles: the populations of the excited atoms, molecules and ions tend to obey equilibrium laws, such as the Boltzmann, Saha and Guldberg Waage laws. Thermal equilibrium calculation of the transport and thermodynamic properties is greatly simplified by comparison with non-equilibrium calculations.

Thermal plasma processing, and in general gas phase syntheses of nanopowders, should be operated at high concentrations that are necessary for the practical fabrication of nanostructured materials in industry. This presents serious difficulties in terms of controlling the size, morphology, crystalline phase, and composition, which ultimately determine the properties of the nanostructured materials. To master and optimize the thermal plasma technologies we should understand not only the mechanisms of generation, growth, and deposition of nanoparticles, but also the fundamental nature of the transport phenomena occurring in the plasma during the synthesis. Modern Computational Fluid Mechanics (CFD) modeling and other computer simulation capabilities such as Monte Carlo methods prove to be not only useful but essential to the task. The control of the thermal plasma technologies, which present extreme gradients of all the properties of interest, requires a good knowledge of nanometer-sized particle generation in terms of size distribution, shape, composition and phase, and also requires the development of methodology to transport and deposit particles at specific locations of interest.

A full theoretical description of the aerosol dynamics in plasma processing is very complex due to the presence of neutral atoms, free electrons and ions, and the presence of large temperature gradients. A complete model for such a system requires the solution of

the coupled system of Maxwell equations with the Navier Stokes, energy and mass transfer equations. To this already very complex model describing the LTE plasma must be added the description of the particulate phases, in other words the micron-sized particles injected in the plasma as feed material and the equations describing the aerosol dynamics produced by the condensation. Among the problems related to the modeling of such production, the calculation of the transport properties is of paramount importance.

In the production of nanoparticles of refractory materials, high temperatures can be obtained from many different high energy sources, such as hydrocarbon flames, laser beam, or Joule heating. Nevertheless, with such techniques, production rates are usually low and therefore industrially restricted to certain types of materials. Plasma reactors in thermal plasma technology mostly refers to the downstream section of the plasma process where the hot gas is quenched to freeze the products in the desired thermodynamic state. The specific characteristics which appeals to material processing and nanopowder production are mostly their high energy density, from 10^6 to 10^7 J/m³, the production of reactive species through rapid chemical kinetics, direct conversion from electric to thermal energy, thus providing a better chemical environment control. Thermal plasma jets produced by dc arcs or RF discharges at pressures close to atmospheric pressure are characterized by high temperatures (typically between 6000 and 14,000 K) of heavy species and medium to high subsonic velocities (from a few tens of meters per second up to a few kilometers per second) of the plasma flow. Nanosized particles will form in the zone of the plasma reactor where gases have cooled considerably (below 3500 K for the high temperature refractories) and vapors can condense, predominantly via homogeneous nucleation.

The thermal plasma synthesis of nanopowders is a relatively new technology which has great industrial potential, although it is almost 30 years ago that Yoshida et al. (Yoshida et al., 1979) reported using rf inductively coupled plasma to produce 10 nm titanium nitride in 1979 and in 1981 (Yoshida and Akashi, 1981), as well as earlier works of Troitskii et al (Troitskii et al., 1974) in 1974 and Cantaloup and Mocellin in 1975 (Cantaloup and Mocellin, 1975). But in spite of these pioneering papers, significant industrial breakthroughs have been lagging behind the early researchers enthusiasm. However, the last decade has seen the interest for nanosized materials grow rapidly and thermal plasma technology has been proven capable of producing high quality powders with relative ease. The ultrafine powders are now labeled in the nanotechnology field and their properties interpreted with new light.

In most processes using thermal plasma processing of nanopowders, the high energy densities of thermal plasmas are used to generate high-density vapor-phase precursors that are rapidly quenched to synthesize nanopowders. In these cases, the thermal plasma synthesis of nanopowders includes the following stages:

1. injection of the solid reactants in the plasma.
2. heating, melting, vaporization, and dissociation of the solid reactant feed into gaseous species.
3. reaction between the gaseous reactant to form a new compound.
4. homogeneous nucleation of the new compound, resulting in nanoscale base particles.

5. Use of rapid quenching to control the evolution of the morphology of the aerosol particles through collisions causing coalescence, aggregation, agglomeration, and formation of complex, fractal shape aggregates.
6. Capture of the nanoparticles by filtration, thermophoretic deposition, liquid scrubbing, ...

In the process of nanopowders synthesis using thermal plasmas, in particular those using evaporation-condensation, the properties of the synthesized particles such as particle size, size distribution, phases and morphology are affected by various process parameters. Gas pressure, plasma power, frequency, flow rates of the different torch gases, size of the precursor powders and powder loading in the plasma are key process parameters since they control in turn the particles and vapors temperature histories in the plasma. In order to optimize and control the process for nanoparticle synthesis, it is necessary to understand the effects of the process parameters on plasma properties and on the plasma-particles interactions resulting in final properties of the synthesized powders. In the following sections, we will address the modeling of the induction thermal plasma torches that are used in the production of nanopowders. The transport and thermodynamic properties of thermal plasmas will be addressed.

1.2 The Inductively Coupled Plasma (ICP)

Thermal plasma generation devices, often called plasma torches, are extremely diversified, but roughly they can be classified in three types:

1. The transferred arc torch and free burning arcs, which produces typically plasma temperatures in the range 10000-20000 K, intermediate plasma velocities, in the 100-500 m/sec, and large plasma volumes. In the free burning arcs and transferred arcs the arc is struck between two electrodes, the anode usually being used as the target which receives most of the heat flux. Transferred arc reactors may vary largely in power, industrial units in the megawatts have been used in the metallurgical industry for decades.
2. The DC plasma torch, where the decaying plasma jet has lower temperatures than the transferred arc, velocities close to or above $Ma=1$ depending on the geometry of the torch and nozzle (often the anode itself), and relatively small plasma volumes. The arc is struck between a pointed tip cathode and an annular anode, it is blown and controlled through the use of the plasma gas flow. The plasma power in industrial DC torches varies from a few kW up to 8 megawatts.
3. The inductively coupled plasma torch (ICPT), which is an electrode-less discharge with relatively low velocities (10-100 m/sec), and temperatures that may vary largely with the type of gas used. This type of torch makes it possible to use (in principle) any plasma gas because of its independence on electrodes. Widely used in spectrochemical analysis in small 1 kw units, industrial inductively coupled plasma torches have been reported close to the megawatt range, and of course the von Karman Institute has an ICP of 1.2 Megawatts.

Combinations of the two main types of arc plasmas, transferred or non transferred, have been used extensively in attempts to combine the raw power of the transferred arc with the control of the plasma jet torch. The first industrial use of thermal arc plasma torches dates as far as 1905, before Langmuir's denomination of physical plasmas, for nitrogen oxide generation using the Birkeland et Eyde process. An impressive power of up to a hundred megawatts is reported to have been used up to 1920, when the process was abandoned. In 1939, Huls developed 8,5 megawatts torches for acetylene production from methane and hydrogen gas.

1.3 ICP production of nanoparticles

The industrial interest in nanoparticle production using thermal plasmas has lead, in the last few years, to a number of scientific papers addressing the possibility of creating various types of materials using thermal plasma technology[3]. It has brought even more studies directed to the design of better plasma reactors, with the size, morphology, chemical and structural aspects of the powders as a function of the operating conditions of the reactors. Flow rates of powders, reactants, quench configuration, plasma power, frequency, reactor pressures and other design parameters have been studied using on-line diagnostic of the plasma reactor, as well as on-line monitoring of the powders. Furthermore, the ICP torch can be quite easily modified to a supersonic configuration materials. The supersonic plasma jet obtained is a useful tool used in the spraying technology to produce high-quality coatings. The supersonic expansion has been used for DC plasma jets for many years and has been shown to improve material processing applications such as plasma spraying and the deposition by thermal evaporation. In fact, the low-pressure supersonic plasma jet is now widely used in plasma spraying to produce high quality coating . This sprayed particles are accelerated and attain a higher impact velocity, leading to a higher density of deposit.

1.4 Plasma properties

The transport properties for thermal plasma are obtained using the Chapman-Enskog method. Using a first-order approximation of the Chapman-Enskog method is rather common in the literature because higher-order approximation of Sonine polynomial expansion requires numerous collision integrals resulting in a heavy, cumbersome formula. The first-order approximation gives reasonable enough at temperatures below 9000 K but becomes increasingly inaccurate especially for electrical conductivity and thermal conductivity of electron translational contribution at high temperature . Therefore, higher-order approximations have to be used in order to obtain better precision.

1.4.1 Thermodynamic properties

For such complex mixtures, the thermodynamic properties as well as the transport properties represent a challenging computational task. However, if the molecular data necessary for calculation of the partition functions is known (energy levels, degeneracies, etc...),

it becomes relatively easily to compute thermodynamic properties through a straightforward procedure. Easily applied mixture rules can then be used to obtain easily the properties of the plasma, once the species concentrations are known. In order to evaluate the thermodynamic properties, one uses statistical thermodynamic:

$$E = \sum_{i=0}^{\infty} \epsilon_i N_i \quad \text{and} \quad N = \sum_{i=0}^{\infty} N_i \quad (1)$$

where N_i is the number of particles of energy level i . If the distribution of N_i is known, it is possible to calculate the energy of the system. For a *Boltzmann distribution*:

$$N_i = \frac{N g_i \exp(-\epsilon_i/k T)}{Q} \quad (2)$$

with

$$Q = \sum_{i=0}^{\infty} g_i \exp(-\epsilon_i/k T) \quad (3)$$

Q is the *partition function*, k Boltzmann's constant and g_i the degeneracy of the level i .

The global partition function Q has the form:

$$Q = \sum_{n=1}^{\infty} \sum_{J=0}^{\infty} \sum_{\nu=0}^{\infty} \sum_{e=0}^{\infty} g_n g_J g_\nu g_e \exp \left[-\frac{(\epsilon_{n,tr} + \epsilon_{J,rot} + \epsilon_{\nu,vib} + \epsilon_{e,elec})}{k_B T} \right] \quad (4)$$

and it can be written as:

$$Q = Q_{tr} Q_{rot} Q_{vib} Q_{elec} \quad (5)$$

where the different modes of energy are identified as the translation, rotation, vibration and electronic modes. The individual partition functions are expressed:

Partition function for translation Q_{tr} :

$$Q_{tr} = \left(\frac{2\pi m k T}{h^2} \right)^{3/2} V \quad (6)$$

V is the volume of the system, m the mass of the species and h Planck's constant.

Partition function for rotation Q_{rot} : If in thermal plasma we consider only diatomic molecules, a very reasonable hypothesis, the internal energy of the rigid rotator is:

$$\epsilon_{J,rot} = \frac{h^2}{8\pi^2 I_C} J(J+1) \quad \text{with} \quad J = 0, 1, 2, 3, \dots \quad (7)$$

where I is the moment of inertia of the molecule, J the quantum number of rotation. The characteristic temperature for rotational energy is defined as θ_R :

$$\theta_R = \frac{hcB_e}{k}, \quad (8)$$

with B_e , a spectral constant, it follows that:

$$Q_{rot} = \frac{T}{\sigma\theta_R} + \frac{1}{3\sigma} + \frac{1}{15\sigma} \frac{\theta_R}{T} \quad (9)$$

σ is a parameter included to take into account for homogeneous and heterogeneous diatomic molecules, it is equal to 2 in the first case and to 1 in the second.

Partition function for vibration Q_{vib} : In a similar way,

$$\epsilon_{\nu,vib} = hf \left(\nu + \frac{1}{2} \right) \quad \text{with} \quad \nu = 0, 1, 2, 3, \dots \quad (10)$$

where f is the frequency of the vibration and ν is the quantum number for vibration, again, defining a temperature for the vibration mode:

$$\theta_V = \frac{hc\omega_e}{k}, \quad (11)$$

we can express the vibration partition function,

$$Q_{vib} = \frac{1}{1 - \exp(-\theta_V T)} \quad (12)$$

Electronic partition function Q_{elec} : Unfortunately, there is no simple formulation for the electronic excitation levels, therefore we come back to the definition, using the characteristic temperature for electronic energy:

$$Q = \sum_{e=0}^{\infty} g_e \exp(-\theta_{E,e}/T) \quad (13)$$

$$\theta_{E,e} = \frac{\epsilon_e}{k} \quad (14)$$

Once the partition functions are evaluated, the evaluation of the thermodynamic properties is straightforward, for example the internal energies and enthalpy:

$$E = Nk_B T^2 \left(\frac{\partial \ln Q}{\partial T} \right)_v \quad (15)$$

Or, simply defining in terms of molar units, we replace the general N with Avogadro's constant N_A :

$$\hat{e} = N_A k_B T^2 \left(\frac{\partial \ln Q}{\partial T} \right)_v = \mathcal{R} T^2 \left(\frac{\partial \ln Q}{\partial T} \right)_v \quad (16)$$

or, replacing \mathcal{R} with R so that

$$R = \frac{\mathcal{R}}{\mathcal{M}}$$

we obtain:

$$e = RT^2 \left(\frac{\partial \ln Q}{\partial T} \right)_v \quad (17)$$

In the same way, molar enthalpy is expressed:

$$\hat{h} = \mathcal{R}T^2 \left(\frac{\partial \ln Q}{\partial T} \right)_v + \mathcal{R}T \quad (18)$$

and in molar units:

$$h = RT^2 \left(\frac{\partial \ln Q}{\partial T} \right)_v + RT \quad (19)$$

1.4.2 Transport properties

Transport properties, on the other hand, are much more complex to evaluate and involve complicated functions of the molecular collision interaction potentials. Their computation involves approximate solutions of the Boltzmann equation through Chapman-Enskog theory. Somehow as the partition function is the fundamental element needed for the calculation of thermodynamic properties, the building block of the transport properties calculation is the collision integral which is described in a formal way as:

$$\Omega_{ij}^{(l,s)*} = \frac{4(l+1)}{(s+1)! [2l+1 - (-1)^l]} \int_0^\infty \int_0^\infty \exp(-\gamma_{ij}^2) \gamma_{ij}^{2s+3} (1 - \cos^l \chi) b db d\gamma_{ij} \quad (20)$$

γ_{ij} is the initial reduced velocity of the colliding molecules i and j :

$$\gamma_{ij} = \sqrt{\frac{\mu_{ij}}{2kT}} g_{ij} \quad (21)$$

g_{ij} is the initial relative velocity of the molecules i and j and μ_{ij} is the reduced mass of molecules i and j :

$$\frac{1}{\mu_{ij}} = \frac{1}{m_i} + \frac{1}{m_j} \quad (22)$$

χ is the angle of deviation of the molecules calculated in the coordinate system of the center of mass of the system:

$$\chi = \pi - 2b \int_{r_m}^\infty \frac{dr/r^2}{\sqrt{1 - [\varphi_{ij}(r) / \frac{1}{2}\mu_{ij}g_{ij}^2] - (b^2/r^2)}} \quad (23)$$

b is the impact parameter. The term r_m is the root of

$$1 - \frac{\varphi_{ij}(r)}{\frac{1}{2}\mu_{ij}g_{ij}^2} - \frac{b^2}{r_m^2} \quad (24)$$

and $\varphi_{ij}(r)$ is the energy potential between the two colliding molecules.

The computation of the collision integral is a considerable task, fortunately some reliable data exists for a few well known systems. For example, one can find the collision integrals for air plasmas in the following reduced form:

$$\Omega_{ij}^{(l,s)*} = \frac{4(l+1)}{(s+1)! [2l+1 - (-1)^l]} \sqrt{\frac{2\pi\mu}{kT}} \Omega_{ij}^{(l,s)} \quad (25)$$

and curve fitted to the following form, the tabulated form (Mason et al., 1967) of the coefficients for a mixture of oxygen and nitrogen are available in the literature:

$$\ln(\Omega^*) = A + B \ln(T) + C \ln^2(T) + D \ln^3(T) + E \ln^4(T) \quad (26)$$

Viscosity η Using the known collision integrals, the calculation of the individual species and of the mixtures' transport properties can be evaluated. The case of viscosity is simpler, since the contribution of electrons can be neglected, but in principle still requires the evaluation of a matrix system. Gupta and his collaborators (Gupta et al., 1991) proposed a formulation using a strong diagonal form with only corrective terms for the extra-diagonal terms. It is expressed as:

$$\eta = \left(\sum_{i=1}^{n_{sp}-1} \frac{x_i}{A_i + a_{av}} \right) \left(1 - a_{av} \sum_{i=1}^{n_{sp}-1} \frac{x_i}{A_i + a_{av}} \right)^{-1} \quad (27)$$

with:

$$a_{av} = \left[\sum_{i=1}^{n_{sp}} \sum_{j=1}^{n_{sp}} x_i x_j \left(\frac{1}{A_i} - \frac{1}{A_j} \right)^2 a_{ij} \right] \left[\sum_{i=1}^{n_{sp}} \sum_{j=1}^{n_{sp}} x_i x_j \left(\frac{1}{A_i} - \frac{1}{A_j} \right)^2 \right]^{-1} \quad (28)$$

$$a_{ij} = \frac{N_A}{M_i + M_j} \left(2\Delta_{ij}^{(1)} - \Delta_{ij}^{(1)} \right) \quad (29)$$

$$A_i = \sum_{j=1}^{n_{sp}} x_j \frac{N_A}{M_i} \Delta_{ij}^{(2)} \quad (30)$$

$$\Delta_{ij}^{(1)} = \frac{8}{3} \Omega_{ij}^{(1,1)*} \left[\frac{2M_i M_j}{\pi R T (M_i + M_j)} \right]^{1/2} \quad (31)$$

$$\Delta_{ij}^{(2)} = \frac{16}{5} \Omega_{ij}^{(2,2)*} \left[\frac{2M_i M_j}{\pi R T (M_i + M_j)} \right]^{1/2} \quad (32)$$

Thermal conductivity λ_{eff} For the case of thermal equilibrium, the thermal conductivity of the thermal plasma is the sum of three components, translational, internal, and reaction:

$$\lambda_{eff} = \lambda_{trans} + \lambda_{int} + \lambda_{rea} \quad (33)$$

Using the fact that electron-ion and electron-atom or molecule collisions do not affect significantly the heavy particles, one can decouple to a certain extent the system:

$$\lambda_{trans} = \lambda_h + \lambda_e \quad (34)$$

Translational thermal conductivity λ_h Using the same technique as for viscosity:

$$\lambda_h = \left(\sum_{i=1}^{n_{sp}-1} \frac{x_i}{A_i + a_{av}} \right) \left(1 - a_{av} \sum_{i=1}^{n_{sp}-1} \frac{x_i}{A_i + a_{av}} \right)^{-1} \quad (35)$$

with:

$$a_{av} = \left[\sum_{i=1}^{n_{sp}-1} \sum_{j=1}^{n_{sp}-1} x_i x_j \left(\frac{1}{A_i} - \frac{1}{A_j} \right)^2 a_{ij} \right] \left[\sum_{i=1}^{n_{sp}-1} \sum_{j=1}^{n_{sp}-1} x_i x_j \left(\frac{1}{A_i} - \frac{1}{A_j} \right)^2 \right]^{-1} \quad (36)$$

$$a_{ij} = \frac{2M_i M_j}{15k (M_i + M_j)^2} \left[\left(\frac{33}{2} - \frac{18}{5} B_{ij}^* \right) \Delta_{ij}^{(1)} - 4\Delta_{ij}^{(2)} \right] \quad (37)$$

$$A_i = \sum_{j=1}^{n_{sp}-1} x_j \frac{2}{15k (M_i + M_j)^2} \left[8M_i M_j \Delta_{ij}^{(2)} + (M_i - M_j) \left(9M_i - \frac{15}{2} M_j + \frac{18}{5} B_{ij}^* M_j \right) \Delta_{ij}^{(1)} \right] \quad (38)$$

$$B_{ij}^* = \frac{5\Omega_{ij}^{(1,2)*} - 4\Omega_{ij}^{(1,3)*}}{\Omega_{ij}^{(1,1)*}} \quad (39)$$

This formulation is not complete but the terms neglected account for thermal diffusion which is at least an of magnitude lower than the other conduction terms.

Translational thermal conductivity of electrons, λ_e (Devoto, 1966) demonstrated that, while a lower order of approximation is sufficient for ions, atoms and small molecules found in plasmas, for electrons it is necessary to use higher orders. A third order approximation is shown below. In fact, when temperatures are such that electron and neutrals dominate, this approximation is still inadequate but since for these conditions $\lambda_h \gg \lambda_e$, and the overall λ_{trans} therefore remains accurate. The formulation of Devoto is given below:

$$\lambda_{electron} = \frac{75n_e^2 k}{8} \left(\frac{2\pi kT}{m_e} \right)^{1/2} \frac{1}{q^{11} - (q^{12})^2 / q^{22}} \quad (40)$$

$$q^{11} = 8\sqrt{2}n_e^2 \Omega_{ee}^{(2,2)*} + 8 \sum_i n_e n_i \left(\frac{25}{4} \Omega_{ei}^{(1,1)*} - 15\Omega_{ei}^{(1,2)*} + 12\Omega_{ei}^{(1,3)*} \right) \quad (41)$$

$$q^{12} = 8\sqrt{2}n_e^2 \left(\frac{7}{4} \Omega_{ee}^{(2,2)*} - 2\Omega_{ee}^{(2,3)*} \right) + 8 \sum_i n_e n_i \left(\frac{175}{16} \Omega_{ei}^{(1,1)*} - \frac{315}{8} \Omega_{ei}^{(1,2)*} + 57\Omega_{ei}^{(1,3)*} - 30\Omega_{ei}^{(1,4)*} \right) \quad (42)$$

$$q^{22} = 8\sqrt{2}n_e^2 \left(\frac{77}{16}\Omega_{ee}^{(2,2)*} - 7\Omega_{ee}^{(2,3)*} + 5\Omega_{ee}^{(2,4)*} \right) + 8 \sum_i n_e n_i \left(\frac{1225}{64}\Omega_{ei}^{(1,1)*} - \frac{735}{8}\Omega_{ei}^{(1,2)*} + \frac{399}{2}\Omega_{ei}^{(1,3)*} - 210\Omega_{ei}^{(1,4)*} + 90\Omega_{ee}^{(1,5)*} \right) \quad (43)$$

Internal thermal conductivity, λ_{int} The contribution of the internal modes of energy (rotation, vibration and electronic levels) are given by the formula:

$$\lambda_m = k \sum_{i=1}^{n_{sp}} \frac{x_i \hat{c}_{p,i}^{(m)}}{\mathcal{R} \sum_{j=1}^{n_{sp}} \sum_{k=1}^{n_{sp}} x_k D_{jk}} \quad (44)$$

with m stands for the internal mode considered. $\hat{c}_{p,i}^{(m)}$ is the constant pressure specific heat per unit mole for species i in mode m .

Reactive conductivity λ_{rea} The coefficients presented do not take into account chemical reactions as such. The method proposed by Butler and Brokaw (1957) and Brokaw (1960) must be used but will not be described here. The thermal conductivity of reaction is defined for equilibrium and represents the energy transferred by the chemical reactions in a temperature gradient. For non-equilibrium the term will not be included as a thermal conductivity but the actual energy flux created will be formulated from the diffusion fluxes in the transport equation.

Electrical conductivity σ In thermal plasmas, the electrical conductivity is largely due to electrons, Devoto proposed a third order approximation which is adequate for the temperature range involved in thermal plasma technology:

$$\sigma = \frac{75e^2 n_e^2}{2kT} \left(\frac{2\pi kT}{m_e} \right)^{1/2} \frac{1}{q^{00} - (q^{01})^2 / q^{11}} \quad (45)$$

o e is the electron charge and q^{00} , q^{01} are defined as:

$$q^{00} = 8 \sum_i n_e n_i \Omega_{ei}^{(1,1)*} \quad (46)$$

$$q^{00} = 8 \sum_i n_e n_i \left(\frac{5}{2}\Omega_{ei}^{(1,1)*} - 3\Omega_{ei}^{(1,2)*} \right) \quad (47)$$

Diffusion coefficients D_{im} In thermal plasmas, due to the presence of the strong gradients, multicomponent diffusion will cause de-mixing and departure from equilibrium composition. Evaluation of the multicomponent diffusion may be made through the formulation of the Stefan-Maxwell equations, Hirschfelder et al. (1964):

$$\sum_{j=1, j \neq i}^{n_{sp}} \frac{x_i x_j}{D_{ij}} \left(\frac{\vec{J}_j}{\rho_j} - \frac{\vec{J}_i}{\rho_i} \right) = \nabla x_i - \frac{\nabla T}{T} \sum_{j=1, j \neq i}^{n_{sp}} \frac{x_i x_j}{D_{ij}} \left(\frac{D_j^T}{\rho_j} - \frac{D_j^T}{\rho_i} \right) \quad (48)$$

Alternative formulation using Fick's law and pseudo-binary diffusion may also be used, but care must be taken in the approximation to account correctly for molar flux conservation Ramshaw (1990).

1.5 CFD equations specific to thermal plasmas

The specific aspects of CFD modeling applied to thermal plasmas are discussed in the following. With computational packages being more and more accessible, engineers and scientists working in the field of thermal plasma are inevitably faced with some extent of mathematical and numerical modeling. The equations presented do not represent a complete mathematical model but rather point out the equations specific to thermal plasma modeling when non-thermal and non-chemical equilibrium are involved. They are presented for an axis-symmetrical system for both LTE and non-LTE (two-temperature in the present case) plasmas and include the electromagnetic coupling specific to inductively coupled plasmas. In the case of transferred arcs and DC torches, the mathematical modeling should also include the plasma-surface sheaths and the transient aspects of the arc movement, this aspect is not covered in the following dealing with the electrodeless ICP.

1.5.1 Thermal equilibrium

The total energy equation is written as :

$$\vec{\nabla} \cdot (\rho H_g \vec{u}) = \vec{\nabla} \cdot \left((\lambda_h + \lambda_e)^{eff} \vec{\nabla} T_g - \sum_j h_j \vec{J}_j + (\bar{\tau}_{eff} \cdot \vec{v}) \right) + \vec{u} \cdot \vec{\nabla} p + P_J + S_h - S_{rad}(T) \quad (49)$$

it is the sum of the energy equations of the heavy particles and electrons. H_g is the total enthalpy and can be defined as follows:

$$H_g = h + \frac{|V|^2}{2} \quad (50)$$

The static enthalpy h is defined for ideal gases as :

$$h = \sum_j Y_j h_j \quad (51)$$

where h_j is the enthalpy of species j :

$$h_j = \int^T c_{p,j} dT \quad (52)$$

$c_{p,j}$ is the specific heat of species j .

1.5.2 Thermal non-equilibrium

As the plasma torches and reactors are often operated at the edge of the thermal equilibrium limits, typically at low pressures, the gradients become more pronounced and

the time scales for establishment of equilibrium between the different energy modes and species populations become larger by comparison with the time scales of the apparatus. The non-equilibrium is more pronounced near the edges of the plasma, for example near the cooled walls or in regions of intense quench. The description of the temperature in these regions becomes problematic since typically the electron temperatures will be higher than that of the other species. A two-temperature description of the plasmas near but not at thermal equilibrium has been proposed by (Mostaghimi et al., 1987) for an argon inductively coupled plasma. The following sections describe a two-temperature model adapted from (Mostaghimi et al., 1987) and use the method of (Park, 1986) to extend it to a chemically reactive multi-species plasma.

Momentum:

$$\begin{aligned} \frac{\partial(\rho uu)}{\partial z} + \frac{1}{r} \frac{\partial(r\rho vu)}{\partial r} &= \frac{\partial}{\partial z} \left(\mu_{eff} \frac{\partial u}{\partial z} \right) \\ &+ \frac{1}{r} \frac{\partial}{\partial r} \left(r\mu_{eff} \frac{\partial u}{\partial r} \right) - \frac{\partial p}{\partial z} + \frac{\partial}{\partial z} \left(\mu_{eff} \frac{\partial u}{\partial z} \right) + \frac{1}{r} \frac{\partial}{\partial r} \left(r\mu_{eff} \frac{\partial v}{\partial z} \right) + F_z \end{aligned} \quad (53)$$

$$\begin{aligned} \frac{\partial(\rho uv)}{\partial z} + \frac{1}{r} \frac{\partial(r\rho vv)}{\partial r} &= \frac{\partial}{\partial z} \left(\mu_{eff} \frac{\partial v}{\partial z} \right) + \frac{1}{r} \frac{\partial}{\partial r} \left(r\mu_{eff} \frac{\partial v}{\partial r} \right) \\ &- \frac{\partial p}{\partial r} + \frac{\partial}{\partial z} \left(\mu_{eff} \frac{\partial u}{\partial r} \right) + \frac{1}{r} \frac{\partial}{\partial r} \left(r\mu_{eff} \frac{\partial v}{\partial r} \right) - 2\mu_{eff} \frac{v}{r^2} + F_r \end{aligned} \quad (54)$$

where u and v are the axial and radial velocities, p is pressure, ρ is the plasma density, F_z and F_r are the axial and the radial components of the Lorentz force, and $\mu_{eff} = \mu_l + \mu_t$ is the effective viscosity, which is the combination of molecular μ_l and turbulent viscosity μ_t .

Energy equation of heavy particles: The so-called heavy particles are the ions, atoms and molecules. The non-equilibrium model used here assumes equilibrium between the heavy particles translational and rotational modes, while the electrons are in equilibrium with the vibrational modes, according to the proposition of (Park, 1986).

$$\begin{aligned} \vec{\nabla} \cdot (\rho H_h \vec{u}) &= \vec{\nabla} \cdot \left(\lambda_h^{eff} \vec{\nabla} T_h \right) + \sum_{j(j \neq e)}^{n_{sp}} \left[\vec{\nabla} \cdot \left(\rho D_i^m h_j \vec{\nabla} Y_j \right) \right] \\ &- \sum_{r(\beta_{er}^f \cdot \beta_{er}^b = 0)}^{n_r} \Delta Q_r + \Phi_\mu + \vec{u} \cdot \vec{\nabla} p_h - P_{el}^{ech} \end{aligned} \quad (55)$$

where λ_h^{eff} is the effective thermal conductivity of heavy particles, which the combination of molecular λ_h and turbulent thermal conductivity λ_{turb} . The molecular thermal conductivity of heavy particles λ_h is defined as follows:

$$\lambda_h = \lambda_h^{tr} + \lambda^{rot} \quad (56)$$

where the members on the right hand side represent, respectively, the translational contribution of heavy particles and the contribution of the rotational modes. The last three terms are, respectively, the viscous dissipation, the pressure work of heavy particles and the energy exchange between heavy particles and electrons by elastic collisions.

Energy equation of the electrons

$$\vec{\nabla} \cdot \left(\frac{5}{2} k_B n_e T_e \vec{u} \right) = \vec{\nabla} \cdot \left(\lambda_e^{eff} \vec{\nabla} T_e \right) - \sum_{r(\beta_{er}^f, \beta_{er}^b \neq 0)}^{n_r} \Delta Q_r - S_{rad}(T_e) \quad (57)$$

$$+ \vec{u} \cdot \vec{\nabla} p_e + P_J + P_{el}^{ech}$$

λ_e^{eff} represent the effective thermal conductivity of electrons, which is represented in this model as the sum of the electron thermal conductivity and the vibrational conductivity. $S_{rad}(T_e)$, $\vec{u} \cdot \vec{\nabla} p_e$, P_J and P_{el}^{ech} are, respectively, the volumetric radiative losses, the electron pressure work, the volumetric Joule heating and the energy exchange between heavy particles and electrons by elastic collisions.

For simplicity, inelastic collisions involving electronic, rotational and vibrational excitation reactions are not taken into account. This may affect plasma behavior at low temperatures but should not be of importance in the core of the plasma.

Mass conservation of species s

$$\rho \vec{u} \cdot \vec{\nabla} Y_s = \vec{\nabla} \cdot \left(\left(\rho D_s^m + \frac{\mu_t}{Sc_t} \right) \vec{\nabla} Y_s \right) + R_s \quad (58)$$

where D_s^m is the effective diffusion coefficient. R_s is the net production rate of species s due to reactions and can be written as :

$$R_s = \mathcal{M}_s \cdot \sum_{r=1}^{n_r} (\nu_s^{b,r} - \nu_s^{f,r}) \left(k_r^f \prod_{k=1}^{n_{sp}} N_k^{\nu_k^{f,r}} - k_r^b \prod_{k=1}^{n_{sp}} N_k^{\nu_k^{b,r}} \right) \quad (59)$$

Under thermal non equilibrium, the reaction rate depend upon the heavy particle temperature as well as the vibrational temperature. This can be a problem when the heavy particle temperature and the vibrational temperature are not equal because we do not know which temperature is controlling the reaction. To treat this problem, we may use Park (1986) multi temperature approach. Using this approach, the backward and forward rate coefficients are evaluated with rate controlling temperature T_r . The forward and backward rate coefficients are evaluated with rate-controlling temperature $T_r = T_f$ and $T_r = T_b$, defined as follows:

$$T_f = T_h^{1-q_f} T_e^{q_f} \quad \text{and} \quad T_b = T_h^{1-q_b} T_e^{q_b} \quad (60)$$

The reaction rate k_r^f for the forward direction is given by the Arrhenius law :

$$k_r^f = a_l T_r^{b_l} \exp(-c_l/T_r). \quad (61)$$

The constants a_l , b_l and c_l are taken from Abeele (2000).

The reaction rates k_r^b for the backward direction are calculated by the relationship:

$$k_r^b = \frac{k_r^f}{K_c^r} \quad (62)$$

where K_c^r , the equilibrium constant is easily calculated from the statistical mechanics, Bottin (1999). It is defined as follows:

$$K_c^r(T) = K_p^r(k_b T)^{-\sum \nu_s^r} \quad (63)$$

$$K_p^r(T) = \exp\left(-\sum_{i=1}^{n_{sp}} \frac{\nu_i^r \hat{\mu}_i^0}{k_B T}\right) \quad (64)$$

The chemical potentials are given by:

$$\hat{\mu}_i^0 = \hat{\mu}_{i,tr}^0 + \hat{\mu}_{i,rot}^0 + \hat{\mu}_{i,vib}^0 + \hat{\mu}_{i,el}^0 \quad (65)$$

where

$$\hat{\mu}_{i,tr}^0 = k_B T_{h,e} \ln p_0 - k_B T_{h,e} \ln \left[\left(\frac{2\pi m_i}{h^2} \right)^{\frac{3}{2}} k_B^{\frac{5}{2}} \right] - \frac{5}{2} k_B T_{h,e} \ln T_{h,e} \quad (66)$$

$$\hat{\mu}_{i,rot}^0 = -k_B T_h \ln \left(\frac{T_h}{\sigma \theta_{rot,i}} \right) - k_B T_h \ln \left(1 + \frac{\theta_{rot,i}}{3T_h} \right) \quad (67)$$

$$\hat{\mu}_{i,vib}^0 = k_B T_e \ln \left[1 - \exp \left(-\frac{\theta_{vib,i}}{T_e} \right) \right] \quad (68)$$

$$\hat{\mu}_{i,el}^0 = -k_B T_e \ln \left[\sum_{e=0}^{\infty} g_e \exp \left(-\frac{\epsilon_{el,i}^e}{k_B T_e} \right) \right] \quad (69)$$

Where $T_{h,e}$ represents T_e if a species i or j is the electron, otherwise T_h .

1.5.3 Auxiliary relations

The model is completed with the usual definitions and constraints:

Total enthalpy of heavy particles

$$H_h = h_h + \frac{|V|^2}{2} \quad (70)$$

with

$$h_h = \sum_{s \neq e} Y_s h_s, \quad h_s = \frac{1}{m_s} \left(\frac{5}{2} k_B T_h \right) \quad (71)$$

Mass fraction

$$Y_j = \frac{m_j n_j}{\rho} \quad (72)$$

Equation of state In order to close the system, the perfect gas law is used to determine the density :

$$\rho = \rho_e + \rho_h \approx \rho_h = \frac{p_h}{r T_h} \approx \frac{p}{r T_h} \quad (73)$$

with

$$r = R \sum_{j=1}^{n_{sp}} \frac{Y_j}{M_j} \quad (74)$$

Charge neutrality (specific to an air plasma)

$$\frac{Y_e}{m_e} = \frac{Y_{N_2^+}}{m_{N_2^+}} + \frac{Y_{O_2^+}}{m_{O_2^+}} + \frac{Y_{N^+}}{m_{N^+}} + \frac{Y_{O^+}}{m_{O^+}} \quad (75)$$

Balance of mass fraction

$$Y_{N_2} = 1 - \sum_{j(j \neq N_2)}^{n_{sp}} Y_j \quad (76)$$

Exchange due to elastic collisions The elastic energy exchange between electrons and heavy particles is computed by a mean collision frequency approach, Charrada et al. (1996) :

$$P_{el}^{ech} = \frac{(3/2)n_e k_B (T_h - T_e)}{\tau_{eh}} \quad (77)$$

where τ_{eh} is the elastic relaxation time, Ferziger and Kaper (1972):

$$\frac{1}{\tau_{eh}} = (8/3) \sum_{j \neq e} \left(\frac{m_e}{m_j} \nu_{ej} \right) \quad (78)$$

with

$$\nu_{ej} = v_{th-e} n_j \bar{\Omega}_{ej}^{11} \quad (79)$$

v_{th-e} is the thermal velocity of electrons and can be calculated by the following expression:

$$v_{th-e} = (8k_B T_e / \pi m_e)^{1/2} \quad (80)$$

1.5.4 Radiation

In general, the effective radiation emission is computed by subtracting spectrally integrated emission and absorption:

$$S_{rad}(T_e) = 4\pi \int_{\lambda} \varepsilon_{\lambda} d\lambda - \int_{\lambda} a_{\lambda} d\lambda \quad (81)$$

An effective net radiation emission coefficient as described by Lowke (1974) may be used, but should be considered as only approximate. The radiation loss function $S_{rad}(T_e)$ was computed by taking account the atomic and ionic spectral lines and continuous spectra. The continuum radiation arises from recombination (free-bound) and bremsstrahlung (free-free) transitions:

$$S_{rad}(T_e) = \frac{4\pi}{(4\pi\epsilon_0)^3} \frac{16\pi e^6}{\sqrt{6\pi m_e^3 k_B}} \sum_{ion} \frac{n_e n_{ion}}{\sqrt{T_e}} z_{ion}^2 \frac{4k_B T_e}{h_p} \quad (82)$$

$$+ \sum_{all-lines} \frac{h_p c}{\lambda_{ki}} n_j \frac{g_k}{U_j} \exp \left[-\frac{E_k}{k_B T_e} \right]$$

1.5.5 Electromagnetic equations: vector potential formulation

The vector potential formulation of Xue et al. (2001) may be used to describe the electromagnetic fields:

$$\nabla^2 A = -\mu_0 (j_{coil} + j_{ind}) \quad (83)$$

where A is the vector potential, j_{coil} is the current density induced in the coil by the voltage applied to the ends of the coil and j_{ind} is the current density developed in the plasma and the coil by the induced electric field. If j_{coil} is given, A can be calculated, since j_{ind} can be expressed in terms of A . Assuming that all the fields A , E and H are sinusoidal with a frequency f in the r.f. plasma, the time variation of A and J can be omitted and the equation (83) remains the same but A and J will not change with time. Assuming that the coil is made of parallel rings (an hypothesis necessary to keep the symmetry, the vector potential A and the electric field E has only an azimuthal component $A = (0, A_\theta, 0)$ and $E = (0, E_\theta, 0)$.

A_θ is a phasor quantity and has a real and an imaginary part :

$$A_\theta = A_{\theta R} + iA_{\theta I} \quad (84)$$

The magnetic field intensity and the electric field can then be determined using:

$$E_\theta = -i\omega A_\theta \quad (85)$$

$$\mu_0 H_z = \frac{1}{r} \frac{\partial}{\partial r} (r A_\theta) \quad (86)$$

$$\mu_0 H_r = -\frac{\partial}{\partial z} (A_\theta) \quad (87)$$

These equations are coupled to the plasma flow and energy equations, through the radial and axial components of the Lorentz force and through the Joule heating rate:

$$F_r = \frac{1}{2} \mu_0 \sigma Re [E_\theta H_z^*] \quad (88)$$

$$F_z = -\frac{1}{2} \mu_0 \sigma Re [E_\theta H_r^*] \quad (89)$$

$$P_J = \frac{1}{2} \sigma Re [E_\theta E_\theta^*] \quad (90)$$

where the superscript * denotes the complex conjugate.

1.6 Application of the equilibrium model model

The model described in the previous section can be used as the basis for modeling a nanoparticle reactor. Injection of the reactants, either as solid precursors or combinations of solid, gas or liquid flows can be considered. In the case of solid precursors, the description of the secondary phase has to be taken into account, heating and evaporation of the precursor, as well as the subsequent transport and diffusion, has to be considered. In particular, when the secondary phase is concentrated enough to produce two-way interactions, as would be the case in many industrial applications, the interaction between the particulate and the plasma phase have to be taken into account (for example using the PSI-Cell algorithm).

1.6.1 Computational domain and boundary conditions

The geometry of a commercial inductively coupled plasma torch is used in this study. A schematic of the calculation domain of the induction plasma torch with the supersonic nozzle and its major components is shown in figure 1. A summary of the plasma operating conditions is presented in table 1. Passing through the convergent-divergent nozzle the plasma flows into the working chamber where partial vacuum. The chamber pressure is $P_{ch} = 5000 Pa$. The outlet static pressure P_{in} is found in the present model to be higher than P_{ch} ; therefore the plasma jet is underexpanded. In the present work, the plasma generation as well as the expansion nozzle and discharge zone, are modeled and simulated.

The vector potential equations are solved only in the discharge region (Zone I), the quartz tube (Zone III and IV), the coil (Zone II) and the outer zone (Zone V).

The mathematical model is solved in the present case using a commercial package (Fluent).

Table 1: Characteristics of the torch, principal dimensions and operating conditions.

$d_0 = 0.00982(m)$	$d_c = 0.003(m)$	$d_{ch} = 0.2(m)$	$d_{ind} = 0.006(m)$
$L = 0.0326(m)$	$L_{ch} = 0.5(m)$	$L_{con} = 0.025(m)$	$L_{tot} = 0.8076(m)$
$r_1 = 0.004(m)$	$r_2 = 0.013(m)$	$R_{ch} = 0.1(m)$	$R_{ext} = 0.12(m)$
$R_{tor} = 0.025(m)$	$Z_1 = 0.05(m)$	$Z_2 = 0.057927(m)$	$Z_3 = 0.09(m)$
$Z_4 = 0.134763(m)$	$\delta_w = 0.0035(m)$	$P_{Ohmic} = 10.7kW$	$f = 3MHz$
$Q_1 = 10^{-4} \frac{Kg}{s}$	$Q_2 = 1.74 * 10^{-3} \frac{Kg}{s}$	$Q_3 = 1.74 * 10^{-3} \frac{Kg}{s}$	

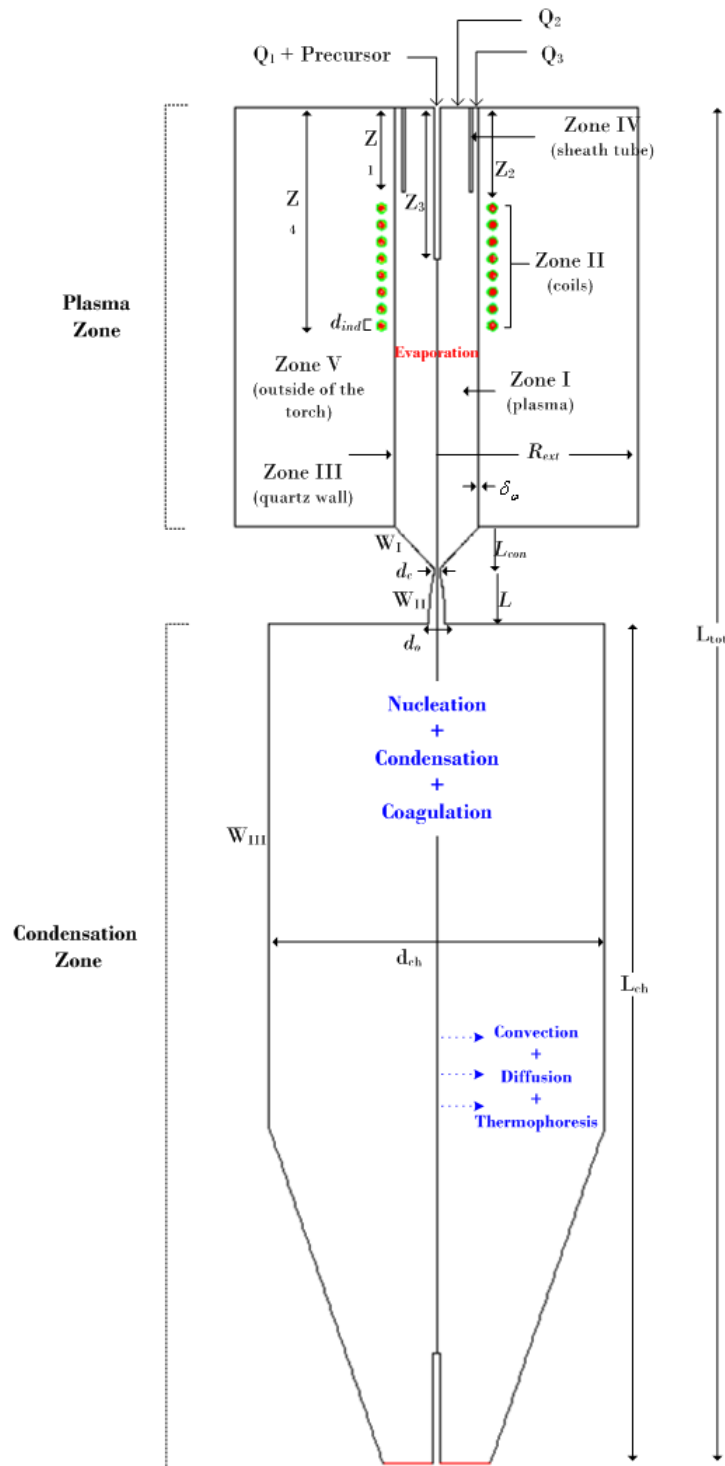


Figure 1: The geometry of the induction plasma torch with the supersonic nozzle

The boundary conditions used are as follows:
At the inlet:

$$Q_1 = 10^{-4}Kg/s, \quad Q_2 = Q_3 = 1.74 * 10^{-3}Kg/s, \quad T = 300K \quad (91)$$

At the wall($r = R_{tor}$):

$$u = v = 0, \quad \frac{\partial(\rho Y_s)}{\partial r} = 0, \quad \lambda \frac{\partial T}{\partial r} = \frac{\lambda_c}{\delta_w}(T - T_{W0}), \quad \frac{\partial T_e}{\partial r} = 0 \quad (92)$$

where $\lambda_c = 1.05W/mK$ is the quartz thermal conductivity and $T_{W0} = 300K$.

At the center($r = 0 m$):

$$\frac{\partial u}{\partial r} = 0, \quad v = 0, \quad \frac{\partial H}{\partial r} = 0, \quad \frac{\partial Y_s}{\partial r} = 0. \quad (93)$$

At the boundaries labeled (W_I, W_{II}):

$$u = 0, \quad v = 0, \quad T = 700K, \quad \nabla \cdot \nabla(\rho Y_s) \cdot \vec{n} = 0 \quad (94)$$

At the boundary labeled (W_{III}):

$$u = 0, \quad v = 0, \quad T = 300K, \quad \nabla(\rho Y_s) \cdot \vec{n} = 0 \quad (95)$$

1.6.2 Results

In the following we examine briefly a few results obtained with the current model applied to the supersonic ICP reactor. First, the temperature and velocity profiles in the discharge region are presented and compared with the case when there is precursor powder present at a relatively small flow rate. It can be observed that the isotherms are displaced downstream due to the two-way coupling. It can also be observed on figures 2 and 3 that the separation occurring on the wall of the plasma torch at the lower part of the coil expands both upstream and downstream.

The iso-concentration of the evaporated silica precursor powder is shown next for two different precursor loading mass rates of 0.3 and 0.9 gpm, on figure 4. Finally, the temperature and Mach number profiles are presented downstream of the plasma torch on figure 5

1.7 Conclusion

A mathematical model of the synthesis of nanoparticles in a radio frequency (RF) inductively coupled plasma (ICP) with a supersonic nozzle is developed. It can be used to describe the flow, temperature, concentration fields of the reactor that is used to produce nanoparticles. The presence of the supersonic nozzle is proposed as a tool to increase the

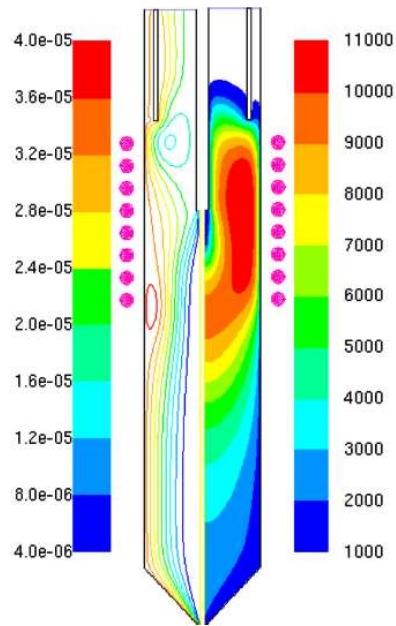


Figure 2: Temperature and stream lines in the discharge without precursor powders

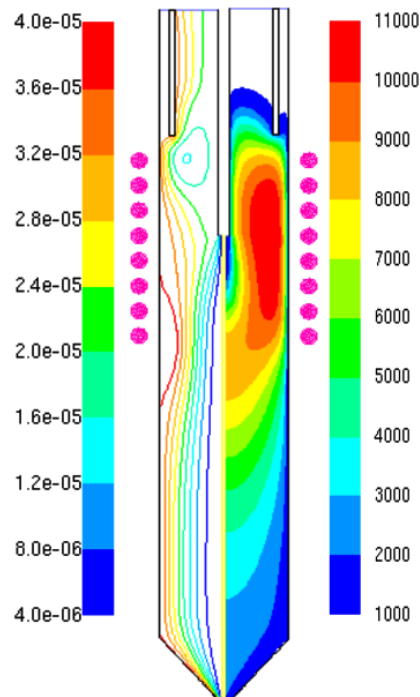


Figure 3: Temperature and stream lines in the discharge with precursor powder (0.9 gpm)

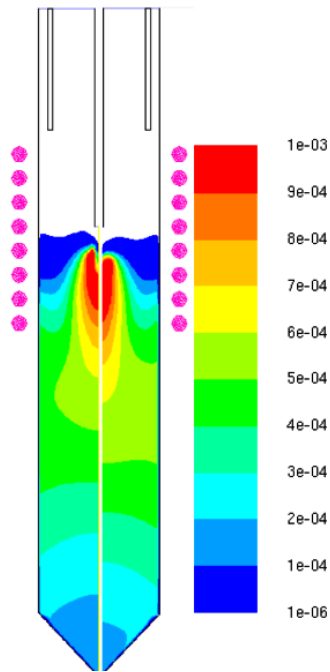


Figure 4: Concentrations of Silica vapor in the discharge region with 0.3 and 0.9 gpm

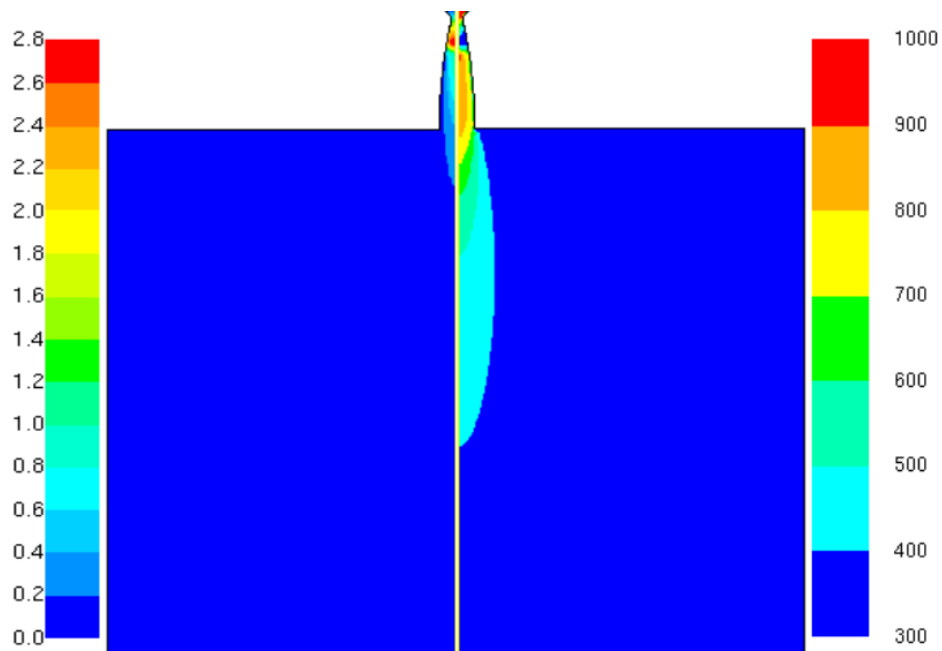


Figure 5: Temperature and Mach number in the nozzle and discharge region

rate of cooling of the flow, thus leading to faster quenching of the nanoparticle distribution. The model can be used in conjunction with the nanoparticle nucleation, coalescence, coagulation and transport models that are further developed and explained in the following sections of the present Lecture Series on Modeling and Computation of Nanoparticles in Fluid Flow. It can further be used in order to optimize the conditions for obtaining nanoparticles of a particular size distribution and morphology, and to understand the complex relationship between the operating conditions of the ICP reactor and the powder produced.

References

- Abeele, D. V. (2000). *An Efficient Computational Model for Inductively Coupled Air Plasma Flows under Thermal and Chemical Non equilibrium*. PhD thesis, Institut Von Karman, Belgique.
- Bottin, B. (1999). *Aerothermodynamic model of an inductively coupled plasma wind tunnel - Numerical and experimental determination of the facility performance*. PhD thesis, Universite de Liege, Liege, Belgium.
- Brokaw, R. (1960). Thermal conductivity of gas mixtures in chemical equilibrium, 2. *Journal of Chemical Physics*, **32**(4): 1005.
- Butler, J. and Brokaw, R. (1957). Thermal conductivity of gas mixtures in chemical equilibrium. *Journal of Chemical Physics*, **26**(6): 1636.
- Cantaloup, J. and Mocellin, A. (1975). *Special Ceramics 6*. P. Popper.
- Charrada, K., Zisis, G., and M., A. (1996). *Journal of physics D: Applied Physics*, **29**: 2432.
- Devoto, R. (1966). Transport properties of ionised monoatomic gases. *Physics of Fluids*, **9**(6): 1230.
- Ferziger, J. H. and Kaper, H. G. (1972). *Mathematical Theory of Transport Processes in Gases*. North-Holland Publishing Company.
- Gupta, R., Lee, K.-P., Thompson, R., and Yos, J. (1991). Calculations and curve fits of thermodynamic and transport properties for equilibrium air to 30000 k. Technical Report 1260, NASA Reference Publication.
- Hirschfelder, J., Curtiss, C., and Bird, R. (1964). *Molecular Theory of Gases and Liquids*. John Wiley & Sons, New York.
- Lowke, J. (1974). Predictions of arc temperature profiles using approximate emission coefficients for radiation losses. *Journal of Quantitative Spectroscopy and Radiative Transfer*, **14**:111.
- Mason, E., Munn, R., and Smith, F. (1967). Transport coefficients of ionized gases. *Physics of Fluids*, **10**(8): 1827.
- Mostaghimi, J., Proulx, P., and Boulos, M. (1987). A two-temperature model of inductively coupled rf plasma. *Journal of Applied Physics*, **61**(5): 1753.
- Park, C. (1986). Assessment of a two temperature kinetic model for dissociating and weakly ionizing nitrogen. Technical Report 86-1347, technical paper, AIAA Boston Massachussets.
- Ramshaw, J. (1990). Self-consistent effective binary diffusion in multicomponent gas mixtures. *Journal of Non-Equilibrium Thermodynamics*, **15**(3): 295.

REFERENCES

REFERENCES

- Troitskii, V., Grebtsov, B., and Aivasov, M. I. (1974). *Sov. Powder Met. Metal Ceram.*, **12**: 869.
- Xue, S., Proulx, P., and Boulos, M. (2001). Extended-field electromagnetic model for inductively coupled plasma. *Journal of Physics D: Applied Physics*, **34**: 1897.
- Yoshida, T. and Akashi, K. (1981). Preparation of ultrafine iron particles using an rf plasma. *Transactions of the Japanese Institute for Metals*, **22**:371–378.
- Yoshida, T., Kawasaki, A., Nakagawa, K., and Akashi, K. (1979). The synthesis of ultrafine titanium nitride in an r.f. plasma. *Journal of Material Science*, **14**:1624–1630.